Vortex Gyroscope Imaging of Planar Superfluids

A. T. Powis, S. J. Sammut, and T. P. Simula

School of Physics, Monash University, Victoria 3800, Australia

We propose a robust imaging technique that makes it possible to distinguish vortices from antivortices in quasi-two-dimensional Bose-Einstein condensates from a single image of the density of the atoms. Tilting the planar condensate prior to standard absorption imaging excites a generalized gyroscopic mode of the condensate, revealing the sign and location of each vortex. This technique is anticipated to enable experimental measurement of the incompressible kinetic energy spectrum of the condensate and the observation of a negative-temperature phase transition of the vortex gas, driven by two-dimensional superfluid turbulence.

Turbulence in classical fluids is one of the most fascinating, yet poorly understood, physical phenomena. The discovery of superfluidity in liquified helium opened new opportunities for understanding the problem from the perspective of quantum turbulence, whose essence is in the dynamics of superfluid vortices and their quantized circulation [1,2]. However, imaging the subnanometer sized cores of the quantized vortices in helium superfluids has remained a significant experimental challenge [3–5].

In dilute gas Bose-Einstein condensates (BECs) the situation is better. Quantized vortices in BECs whose micrometer scale cores are void of condensate particles can be imaged directly by optical means [6–12]. In two-dimensional systems, or in the case of parallel vortex filaments, top-view imaging of the condensate exposes the vortices as pointlike objects with circular nonzero-size cores. Under such conditions, Onsager's statistical hydrodynamical model of turbulence [1] is anticipated to be particularly relevant. Therefore the BECs of dilute gases are ideally suited for studies of two-dimensional superfluid turbulence and the underlying chaotic dynamics of the pointlike vortices and antivortices. Indeed, rapid progress has been made in experimental techniques for studying the dynamics of vortices and quantum turbulence in dilute BECs [13–19].

The locations of vortices in Bose-Einstein condensates can be routinely measured by imaging the spatial density distribution of the condensate atoms. A condensate with a vortex can also be combined with a uniform-phase reference condensate to produce an interferogram. This results in a telltale forked interference pattern from which the direction of the superflow around the vortex core can be determined [20]. Although such interferometric methods are ideally suited for detecting vortices in exciton-polariton systems [21,22], in turbulent atomic BECs such a method is complicated by the requirement of a phase reference condensate. Recently, Donadello *et al.* [23] successfully measured the signs of solitonic vortices [23,24] using a method of twisted densities. However, detecting the

direction of the fluid circulation around the vortex cores of a generic many-vortex configuration has remained difficult to achieve. This is an issue because, unlike steadily rotating superfluids, turbulent systems are not polarized and contain both vortices and antivortices. This vortex circulation sign problem prevents the reconstruction of the superfluid velocity field from experimental data, which holds key information about the turbulent state.

Here we introduce vortex gyroscope imaging (VGI)—a method that enables simultaneous detection of the locations and signs of multiple quantized vortices in a BEC using only a single image of the particle density. This robust method is based on excitation of a gyroscopic BEC tilting mode [25–27] generalized to systems with both vortices and antivortices. Implementation of VGI in experiments can be accomplished with existing technologies. In particular, the VGI method enables direct experimental measurement of the incompressible kinetic energy spectrum of a two-dimensional quantum gas and quantification of the negative-temperature phase transition [28,29] with the associated Onsager vortex states of quantum turbulence [1,29,30].

The elementary principle of the VGI method is illustrated in Fig. 1. The condensate with a vortex, indicated by the red arrow in Fig. 1(a), initially lies at an angle θ_0 with respect to the imaging axis, shown as a vertical dashed line. An absorption image taken of this condensate would reveal both a vortex or an antivortex as a near-circular shadow in the condensate column density, Fig. 1(c). Initially, the small apparent asymmetry of the vortex core depends on the angle subtended by the ends of the vortex line from the imaging device. Quantum mechanically, tilting the condensate, Fig. 1(b), at a sufficient rate excites the first axial Kelvin mode of the vortex. Classically, the torque applied to the vortex gyroscope causes it to precess. When imaged along an axis perpendicular to the condensate plane, the vortex is now observed as an elliptical shadow, Fig. 1(d), whose semimajor axis rotates at frequency ω_1 in a direction determined by the sign of the vortex circulation vector $\boldsymbol{\kappa}$.
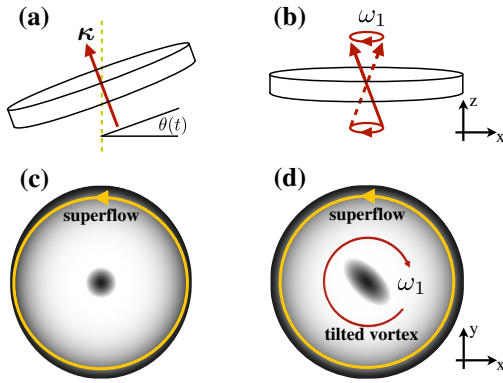
FIG. 1 (color online). Schematic of the vortex gyroscope imaging method for detecting the sign of the quantized circulation of vortices in Bose-Einstein condensates.

Kelvin waves [31–39] have a negative helicity, and therefore the direction of the condensate superflow and the observed gyroscopic motion of the tilted vortex are in opposite directions. Importantly, this means that the elliptical shadows corresponding to a vortex and an antivortex will precess in opposite directions. Capturing an absorption image after these ellipses have rotated by $\pi/4$ rad, the timing of which is governed by the gyroscopic mode frequency ω_1, the semiaxes of the vortex and antivortex ellipses will be perpendicular and clearly distinguishable.

A similar tilting technique has been used in experiments with a single vortex to excite the scissors mode [40,41], and to observe the gyroscopic Kelvin-Tkachenko mode of a polarized vortex array [25–27], which involves three-dimensional motion of the vortices in contrast to the purely transverse fundamental Tkachenko mode [42–50]. In another experiment, Bretin et al. [51] excited a higher Kelvin wave number of a single vortex [37,38,52]. The VGI method amounts to the excitation of a generalized gyroscopic mode in which each vortex precesses about its localized position in the direction determined by the sign of their circulation.

We model harmonically trapped BECs using the Gross-Pitaevskii equation [32,53]

$$i\hbar \frac{\partial \psi(\mathbf{r}, t)}{\partial t} = \left(-\frac{\hbar^2}{2m} \nabla^2 + V_{\mathrm{trap}}(\mathbf{r}, t) + g|\psi(\mathbf{r}, t)|^2 \right) \psi(\mathbf{r}, t),$$
(1)

where the coupling constant $g = 4\pi\hbar^2 a/m$ is determined by the s-wave scattering length a and the particle mass m. The normalization of the condensate wave function $\psi(\mathbf{r}, t)$ determines the number of condensate atoms, $N = \int |\psi(\mathbf{r}, t)|^2 d\mathbf{r}$. The condensate is trapped in a harmonic potential $V_{\mathrm{trap}}(\mathbf{r}) = \frac{1}{2}m(\omega_x^2 x^2 + \omega_y^2 y^2 + \omega_z^2 z^2)$, where the harmonic oscillator frequencies ω_i define a trap with axial symmetry $\omega_x = \omega_y = \omega_\perp$ and an aspect ratio $\lambda = \omega_z/\omega_\perp$. In the results presented, following Neely et al. [14], we have chosen $\lambda = 11.25$, unless otherwise stated. The effect of particle interactions can be parametrized by the dimensionless constant $C = N\sqrt{128}\pi a/a_0$, where $a_0 = \sqrt{\hbar/m\omega_\perp}$ is the transverse

harmonic oscillator length. For example, choosing our typical parameters $C = 18\,640$ and considering ^{87}Rb atoms with $m = 1.44 \times 10^{-25}$ kg, $a = 5.45$ nm and $\omega_\perp = 2\pi \times 8$ Hz, corresponds to approximately $N = 3.67 \times 10^5$ condensate atoms.

Initially, the z axis of the trap forms an angle θ_0 with respect to the condensate imaging axis. The trap is then smoothly tilted through angle θ_0 during a time $T_{\mathrm{tilt}} = \theta_0/\omega_{\mathrm{tilt}}$. The form of the tilt function was chosen to be

$$\theta(t) = \theta_0[1 - t/T_{\mathrm{tilt}} + \sin(2\pi t/T_{\mathrm{tilt}})/2\pi],$$
(2)

which ensures a continuous and smooth tilt of the trap. Tilting the trap slowly with respect to the time scale set by the trapping frequencies will suppress excessive excitation of sound waves; however, if tilting occurs too slowly, the vortices will adiabatically realign with the condensate axis of symmetry and the vortex gyroscopes will not be excited. The tilt should also occur diabatically [54] such that the locations of the vortices do not change appreciably during the tilting process. The visibility of each vortex ellipse depends on the trapping and tilting parameters in a nontrivial way. We have considered a wide range of tilting parameters to optimize the VGI method, as detailed in the Supplemental Material [55]. The results presented in the main text are obtained for $\theta_0 = \pi/9$ rad and $\omega_{\mathrm{tilt}} = \theta_0\omega_\perp$.

The sequence of our numerical experiment commences with solving for the condensate ground state, followed by imprinting a chosen number of quantized vortices and antivortices in the complex valued wave function. The condensate is then evolved in real time to allow relaxation of the superfluid velocity field. The trap is next tilted to energize the vortex gyroscopes. An integrated column density of the condensate is measured in correspondence with an experimental absorption imaging. This is performed at an optimal time when each vortex has precessed $\pi/4$ rad, after the start of the tilt. We utilize an ellipse-detection algorithm at the location of each vortex core to determine their orientation in the column-density image. Note that at the start of the trap tilt, all vortex ellipses are initially polarized in the direction determined by the tilt axis. If the vortices start precessing at a constant rate immediately when the tilting begins, the optimal trap-tilting frequency would be $\omega_{\mathrm{tilt}} = (2\theta_0/\pi^2)\omega_1$ with image acquisition after $T_{\mathrm{tilt}} = \pi^2/2\omega_1$. However, using a fixed tilting angle $\theta_0 = \pi/9$ rad and frequency $\omega_{\mathrm{tilt}} = \theta_0\omega_\perp$ works quite well for our typical trap parameters and a large range of particle numbers [55].

We first compare the vortex precession frequencies measured using the VGI method with a theoretical estimate based on the semiclassical Kelvin wave dispersion relation [31,56]

$$\omega_q(k_q) = \frac{\hbar}{mr_c^2}\left(\sqrt{1 + k_q r_c \frac{K_0(k_q r_c)}{K_1(k_q r_c)}} - 1 \right),$$
(3)

where we have substituted the classical circulation with a quantum of circulation $\kappa = h/m$, $r_c = s\xi$ is the vortex core

parameter proportional by a factor of s to the healing length ξ, k_q is the wave vector, and K_ν is a modified Bessel function of the second kind of order ν. The excitation frequency ω_1 of the Kelvin mode with one node is estimated by an effective wave vector $k_1 = s\pi/R_z$, where $R_z = \sqrt{2\mu/m\omega_z^2}$ is the axial Thomas-Fermi (TF) length determined by the local chemical potential $\mu = \mu_{\text{TF}}(1 - r^2/R_\perp^2)$, where $\mu_{\text{TF}} = (15C\lambda/64\pi)^{2/5}\hbar\omega_\perp$ and $R_\perp = \sqrt{2\mu_{\text{TF}}/m\omega_\perp^2}$ is the Thomas-Fermi radius. The local value of the healing length is approximated by $\xi = \hbar/\sqrt{2m\mu}$.

Figure 2(a) shows the measured angular precession frequencies of the vortex gyroscopes as a function of their radial position in the condensate, measured in units of the transverse Thomas-Fermi radius $R_\perp$. The displayed data are obtained for condensates with $N = 1.83 \times 10^5$, and the solid line is the prediction of Eq. (3) using $s = 0.60$. This result shows that the precession frequency of the vortex gyroscopes can be accurately predicted using the single-vortex Kelvin wave dispersion relation [36,55]. More importantly, it shows that the variation in the precession frequency is small across the whole condensate area despite large local density variations. This is crucial for the robust operation of the VGI method in that it allows the simultaneous detection of vortex sign for all vortices from a single absorption image.

Figure 2(b) shows the precession frequencies of the vortex gyroscopes as a function of the chemical potential μ at the locations of the vortices. This includes measurements from condensates with a large range of particle number N and a variety of spatial vortex configurations. The solid line is the theory prediction, Eq. (3), with $s = 0.54$. The data corresponding to Fig. 2(a) is highlighted with triangular markers. Factors contributing to the deviation of the data from the semiclassical Kelvin dispersion relation include the variation of the regularization factor s of the vortex core structure with changing μ, the local density approximation, and the uncertainty of the frequency measurement from the orientation of each vortex ellipse.

Furthermore, Fig. 2(c) shows that the precession frequency as a function of the trap aspect ratio λ for a fixed particle number $N = 1.83 \times 10^5$ is in good agreement with the Kelvin dispersion relation. For $\lambda = \sqrt{8}$ and $N = 7.5 \times 10^4$ Smith et al. [25] observed the tilting mode of a vortex array with the frequency $\omega_1 = 0.33\omega_z$, and for $N = 3 \times 10^4$ the Bogoliubov–de Gennes equations predict $\omega_1 \approx 0.38\omega_z$ for this gyroscope mode [27]. The agreement between the measured vortex gyroscope frequencies ω_1 and Eq. (3) is useful for predicting and calibrating the timing of the image acquisition in experiments [55].

To further corroborate the performance of the VGI method, Fig. 3 shows three examples of a simulated experiment. The rows Figs. 3(a)–3(c), 3(d)–3(f), and 3(g)–(i) correspond to condensates of different particle numbers
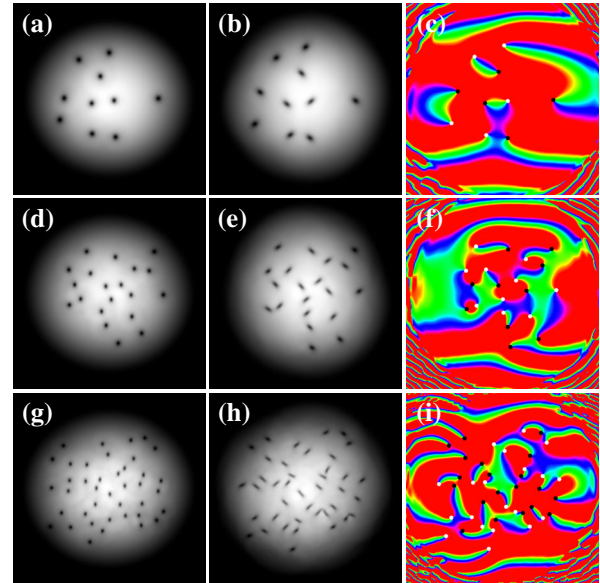
FIG. 3 (color online). Simulated experiments to measure the signs of the vortex circulations using the VGI method. The condensate column density is shown prior to tilting the trap (a),(d),(g) and at the optimal measurement time (b),(e),(h), together with the phase map of the condensate (c),(f),(i) corresponding to respective frames (b),(e),(h). The vortices and antivortices are marked in (c),(f),(i) with black and white circles, respectively. The rows (a)–(c), (d)–(f), and (g)–(i) are for different condensate particle numbers $N \approx (2, 4, 8) \times 10^5$. The images in (b),(e),(h) are obtained at times (13, 13, and 14) ms after the start of the tilt. The fields of view in (a)–(c), (d)–(f), and (g)–(i) are, respectively, (70×70), (81×81), and (94×94) μm.

FIG. 2 (color online). Precession frequencies of the singly quantized vortex gyroscopes, measured using the VGI method, in harmonically trapped Bose-Einstein condensates as functions of (a) the radial vortex location, (b) chemical potential, and (c) the axial trap frequency. The solid line in (a)–(c) corresponds to the theoretical prediction, Eq. (3), based on the Thomas-Fermi approximation with $s = (0.60, 0.54, 0.37)$, respectively.

$N \approx (2, 4, 8) \times 10^5$, respectively. Note the shrinking size of the vortex cores as the condensate density is increased. In the first column [Figs. 3(a), 3(d), and 3(g)] we show the condensate column density prior to commencing the tilt. In the second column [Figs. 3(b), 3(e), and 3(h)] we show the condensate at the optimal measurement time, and in the last column [Figs. 3(c), 3(f), and 3(i)] we show the phase of the complex valued condensate wave function with vortices and antivortices marked at the phase singularities. Note in particular how each vortex sign and position can be inferred from a single measurement [Figs. 3(b), 3(e), and 3(h)] and how little the vortex positions have changed during the tilting procedure. Movies corresponding to these three simulations are included in the Supplemental Material [55].

Having demonstrated the operation of the VGI method, we show how this technique is anticipated to open a path for experimental measurements of the incompressible kinetic energy spectra of quasi-two-dimensional superfluids. Figure 4(a) shows an example of a condensate column density with VGI under turbulent conditions. The vortices and antivortices are imprinted at random locations in the condensate. Both the positions and signs of circulation of all vortices well inside the Thomas-Fermi radius can clearly be inferred from this single image. Following Bradley and Anderson [57], an estimate for the incompressible kinetic energy spectrum $E_i(k)$ of the condensate with N_v vortices can be calculated from

$$E_i(k) = E_0 r_c f(kr_c) \sum_{p=1,q=1}^{N_v} s_p s_q J_0(k|\mathbf{r}_p - \mathbf{r}_q|), \qquad (4)$$

where $E_0 = L\kappa^2\rho_s/2\pi$, L is the effective thickness of the condensate, $\rho_s = m\mu/g$, and s_p and $\mathbf{r}_p$ are the respective sign and position of vortex p with circulation $s_p\kappa$. The function $f(z) = z/4[I_1(z/2)K_0(z/2) - I_0(z/2)K_1(z/2)]^2$, where J_ν and I_ν are the order ν Bessel function and the modified Bessel function of the first kind [57].

The spectrum of Eq. (4) is shown in Fig. 4(b) as a function of the wave vector k. The dashed curve corresponds to the data measured from frame Fig. 4(a) and the thick solid curve is an ensemble average composed of 1000 randomly generated vortex configurations. Figures 4(c) and 4(d) correspond to an Onsager vortex state [29] where the vortex gas has undergone a negative-temperature phase transition and the vortices and antivortices have been separated into two clusters, forming a supervortex dipole. A clear signature of the spectral Einstein-Bose condensation to the Onsager vortex state [1,29,30,58] is highlighted by the shaded region in Fig. 4(d), where the thick and thin solid curves correspond to ensemble averages of 1000 randomly distributed uniform and clustered vortex configurations, respectively. This data show that by using VGI the incompressible kinetic energy spectra and the negative-temperature Onsager vortex phase are detectable even from single absorption images of the condensate density.

In conclusion, we have shown that the vortex gyroscope imaging method, whereby tilting a quasi-two-dimensional superfluid excites the generalized gyroscopic mode of the system, can be used to detect both the sign and location of quantized vortices from a single absorption image of the superfluid. The VGI method also allows for reconstruction of the spatial phase of the condensate and is anticipated to open a pathway for experimental measurements of the incompressible kinetic energy spectra and the negative-temperature Onsager vortex states in quantum turbulent planar superfluids. The VGI method is ideally suited to in-trap imaging of vortices in quasi-two-dimensional superfluids [12], where Crow instability [59] is suppressed and the energies of the lowest Kelvin excitations are high in comparison to the characteristic temperature of the system [60]. However, it could also be combined with time-of-flight imaging [55]. Intriguingly, the VGI method may also enable direct observation of the bound vortex-antivortex pairs inherent to the Hauge-Hemmer-Berezinskii-Kosterlitz-Thouless mechanism [61–68].
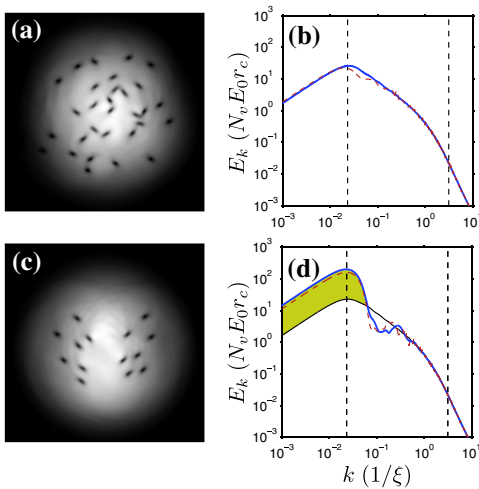
FIG. 4 (color online). Spectral signatures of quantum turbulent quasi-two-dimensional Bose-Einstein condensates with $N = 3.67 \times 10^5$. The condensate column density after the application of VGI is shown for two vortex configurations (a) and (c). The corresponding angle-averaged incompressible kinetic energy spectra (dashed red curves), calculated using Eq. (4), are shown in (b) and (d). The solid thick curves correspond to ensemble averages of randomly sampled uniform (b) and clustered (d) vortex configurations. The thin solid curve in (d) is an ensemble average of random uniform-vortex configurations. The signature of Einstein-Bose condensation of Onsager vortices in this system is highlighted in (d). The vertical dashed lines mark the locations $k_R = \pi/R_\perp$ and $k_\xi = \pi/\xi$. The field of view in (a) and (c) is (81×81) μm.

[1] L. Onsager, Nuovo Cimento **6**, 279 (1949).
[2] R. P. Feynman, Prog. Low Temp. Phys. **1**, 17 (1955).
[3] E. J. Yarmchuk, M. J. V. Gordon, and R. E. Packard, Phys. Rev. Lett. **43**, 214 (1979).
[4] G. P. Bewley, D. P. Lathrop, and K. R. Sreenivasan, Nature (London) **441**, 588 (2006).

[5] E. Fonda, D. P. Meichle, N. T. Ouellette, S. Hormoz, and D. P. Lathrop, Proc. Natl. Acad. Sci. U.S.A. **111**, 4707 (2014).

[6] M. R. Matthews, B. P. Anderson, P. C. Haljan, D. S. Hall, C. E. Wieman, and E. A. Cornell, Phys. Rev. Lett. **83**, 2498 (1999).

[7] K. W. Madison, F. Chevy, W. Wohlleben, and J. Dalibard, Phys. Rev. Lett. **84**, 806 (2000).

[8] P. C. Haljan, I. Coddington, P. Engels, and E. A. Cornell, Phys. Rev. Lett. **87**, 210403 (2001).

[9] J. R. Abo-Shaeer, C. Raman, J. M. Vogels, and W. Ketterle, Science **292**, 476 (2001).

[10] E. Hodby, G. Hechenblaikner, S. A. Hopkins, O. M. Maragò, and C. J. Foot, Phys. Rev. Lett. **88**, 010405 (2001).

[11] P. Rosenbusch, V. Bretin, and J. Dalibard, Phys. Rev. Lett. **89**, 200403 (2002).

[12] K. E. Wilson, Z. L. Newman, J. D. Lowney, and B. P. Anderson, arXiv:1405.7745.

[13] E. A. L. Henn, J. A. Seman, G. Roati, K. M. F. Magalhaes, and V. S. Bagnato, Phys. Rev. Lett. **103**, 045301 (2009).

[14] T. W. Neely, E. C. Samson, A. S. Bradley, M. J. Davis, and B. P. Anderson, Phys. Rev. Lett. **104**, 160401 (2010).

[15] D. V. Freilich, D. M. Bianchi, A. M. Kaufman, T. K. Langin, and D. S. Hall, Science **329**, 1182 (2010).

[16] T. W. Neely, A. S. Bradley, E. C. Samson, S. J. Rooney, E. M. Wright, K. J. H. Law, R. Carretero-González, P. G. Kevrekidis, M. J. Davis, and B. P. Anderson, Phys. Rev. Lett. **111**, 235301 (2013).

[17] R. Navarro, R. Carretero-González, P. J. Torres, P. G. Kevrekidis, D. J. Frantzeskakis, M. W. Ray, E. Altuntas, and D. S. Hall, Phys. Rev. Lett. **110**, 225301 (2013).

[18] A. C. White, B. P. Anderson, and V. S. Bagnato, Proc. Natl. Acad. Sci. U.S.A. **111**, 4719 (2014).

[19] W. J. Kwon, G. Moon, J.-y. Choi, S. W. Seo, and Y.-i. Shin, arXiv:1403.4658.

[20] F. Chevy, K. W. Madison, V. Bretin, and J. Dalibard, Phys. Rev. A **64**, 031601(R) (2001).

[21] K. G. Lagoudakis, M. Wouters, M. Richard, A. Baas, I. Carusotto, R. André, Le Si Dang, and B. Deveaud-Plédran, Nat. Phys. **4**, 706 (2008).

[22] G. Roumpos, M. D. Fraser, A. Löffler, S. Höfling, A. Forchel, and Y. Yamamoto, Nat. Phys. **7**, 129 (2011).

[23] S. Donadello, S. Serafini, M. Tylutki, L. P. Pitaevskii, F. Dalfovo, G. Lamporesi, and G. Ferrari, Phys. Rev. Lett. **113**, 065302 (2014).

[24] M. J. H. Ku, W. Ji, B. Mukherjee, E. Guardado-Sanchez, L. W. Cheuk, T. Yefsah, and M. W. Zwierlein, Phys. Rev. Lett. **113**, 065301 (2014).

[25] N. L. Smith, W. H. Heathcote, J. M. Krueger, and C. J. Foot, Phys. Rev. Lett. **93**, 080406 (2004).

[26] T. P. Simula and K. Machida, Phys. Rev. A **82**, 063627 (2010).

[27] T. Simula, Phys. Rev. A **87**, 023630 (2013).

[28] J. A. Viecelli, Phys. Fluids **7**, 1402 (1995).

[29] T. Simula, M. J. Davis, and K. Helmerson, Phys. Rev. Lett. **113**, 165302 (2014).

[30] T. P. Billam, M. T. Reeves, B. P. Anderson, and A. S. Bradley, Phys. Rev. Lett. **112**, 145301 (2014).

[31] W. Thomson, Philos. Mag. **10**, 155 (1880).

[32] L. P. Pitaevskii, Zh. Eksp. Teor. Fiz. **40**, 646 (1961) [Sov. Phys. JETP **13**, 451 (1961)].

[33] A. L. Fetter, Phys. Rev. **162**, 143 (1967).

[34] R. J. Donnelly, *Quantized Vortices in Helium II* (Cambridge University Press, Cambridge, England, 1991).

[35] T. Isoshima and K. Machida, Phys. Rev. A **59**, 2203 (1999).

[36] A. L. Fetter, Phys. Rev. A **69**, 043617 (2004).

[37] T. P. Simula, T. Mizushima, and K. Machida, Phys. Rev. Lett. **101**, 020402 (2008).

[38] T. P. Simula, T. Mizushima, and K. Machida, Phys. Rev. A **78**, 053604 (2008).

[39] L. Koens, T. P. Simula, and A. M. Martin, Phys. Rev. A **87**, 063614 (2013).

[40] S. Stringari, Phys. Rev. Lett. **86**, 4725 (2001).

[41] E. Hodby, S. A. Hopkins, G. Hechenblaikner, N. L. Smith, and C. J. Foot., Phys. Rev. Lett. **91**, 090403 (2003).

[42] V. K. Tkachenko, Zh. Eksp. Teor. Fiz. **49**, 1875 (1965) [Sov. Phys. JETP **22**, 1282 (1966)]; **50**, 1573 (1966) [Sov. Phys. JETP **23**, 1049 (1966)]; **56**, 1763 (1969) [Sov. Phys. JETP **29**, 245 (1969)].

[43] I. Coddington, P. Engels, V. Schweikhard, and E. A. Cornell, Phys. Rev. Lett. **91**, 100402 (2003).

[44] G. Baym, Phys. Rev. Lett. **91**, 110402 (2003).

[45] T. P. Simula, A. A. Penckwitt, and R. J. Ballagh, Phys. Rev. Lett. **92**, 060401 (2004).

[46] M. Cozzini, L. P. Pitaevskii, and S. Stringari, Phys. Rev. Lett. **92**, 220401 (2004).

[47] T. Mizushima, Y. Kawaguchi, K. Machida, T. Ohmi, T. Isoshima, and M. M. Salomaa, Phys. Rev. Lett. **92**, 060407 (2004).

[48] L. O. Baksmaty, S. J. Woo, S. Choi, and N. P. Bigelow, Phys. Rev. Lett. **92**, 160405 (2004).

[49] E. B. Sonin, Phys. Rev. A **71**, 011603(R) (2005).

[50] T. Simula, J. Phys. Condens. Matter **25**, 285602 (2013).

[51] V. Bretin, P. Rosenbusch, F. Chevy, G. V. Shlyapnikov, and J. Dalibard, Phys. Rev. Lett. **90**, 100403 (2003).

[52] T. Mizushima, M. Ichioka, and K. Machida, Phys. Rev. Lett. **90**, 180401 (2003).

[53] E. P. Gross, Nuovo Cimento **20**, 454 (1961).

[54] S. M. M. Virtanen, T. P. Simula, and M. M. Salomaa, Phys. Rev. Lett. **87**, 230403 (2001).

[55] See Supplemental Material at http://link.aps.org/supplemental/10.1103/PhysRevLett.113.165303 for movies and further details of the VGI method.

[56] See page 29 in Ref. [34].

[57] A. S. Bradley and B. P. Anderson, Phys. Rev. X **2**, 041001 (2012).

[58] R. H. Kraichnan, Phys. Fluids **10**, 1417 (1967).

[59] T. P. Simula, Phys. Rev. A **84**, 021603(R) (2011).

[60] S. J. Rooney, P. B. Blakie, B. P. Anderson, and A. S. Bradley, Phys. Rev. A **84**, 023637 (2011).

[61] E. H. Hauge and P. C. Hemmer, Phys. Norv. **5**, 209 (1971).

[62] V. L. Berezinskii, Zh. Eksp. Teor. Fiz. **59**, 907 (1971) [Sov. Phys. JETP **32**, 493 (1971)]; Zh. Eksp. Teor. Fiz. **61**, 1144 (1972) [Sov. Phys. JETP **34**, 610 (1972)].

[63] J. M. Kosterlitz and D. J. Thouless, J. Phys. C **6**, 1181 (1973).

[64] T. P. Simula and P. B. Blakie, Phys. Rev. Lett. **96**, 020404 (2006).

[65] Z. Hadzibabic, Z. Krüger, M. Cheneau, B. Battelier, and J. Dalibard, Nature (London) **441**, 1118 (2006).

[66] T. P. Simula, M. J. Davis, and P. B. Blakie, Phys. Rev. A **77**, 023618 (2008).

[67] P. Cladé, C. Ryu, A. Ramanathan, K. Helmerson, and W. D. Phillips, Phys. Rev. Lett. **102**, 170401 (2009).

[68] J. Y. Choi, S. W. Seo, and Y. I. Shin, Phys. Rev. Lett. **110**, 175302 (2013).